Genus Zero Surface Conformal Mapping and Its Application to Brain Surface Mapping

Xianfeng Gu[1], Yalin Wang[2], Tony F. Chan[2], Paul M. Thompson[3], and
Shing-Tung Yau[4]

[1] Division of Engineering and Applied Science, Harvard University
gu@eecs.harvard.edu
[2] Mathematics Department, UCLA
{ylwang,chan}@math.ucla.edu
[3] Laboratory of Neuro Imaging and Brain Research Institute
UCLA School of Medicine
thompson@loni.ucla.edu
[4] Department of Mathematics, Harvard University
yau@math.harvard.edu

Abstract. It is well known that any genus zero surface can be mapped
conformally onto the sphere and any local portion thereof onto a disk.
However, it is not trivial to find a general method which finds a conformal
mapping between two general genus zero surfaces. We propose a new
variational method which can find a unique mapping between any two
genus zero manifolds by minimizing the harmonic energy of the map. We
demonstrate the feasibility of our algorithm by applying it to the cortical
surface matching problem. We use a mesh structure to represent the brain
surface. Further constraints are added to ensure that the conformal map
is unique. Empirical tests on MRI data show that the mappings preserve
angular relationships, are stable in MRIs acquired at different times, and
are robust to differences in data triangulation, and resolution. Compared
with other brain surface conformal mapping algorithms, our algorithm
is more stable and has good extensibility.

1 Introduction

Recent developments in brain imaging have accelerated the collection and
databasing of brain maps. Nonetheless, computational problems arise when inte-
grating and comparing brain data. One way to analyze and compare brain data
is to map them into a canonical space while retaining geometric information on
the original structures as far as possible [1,2,3,4,5]. Fischl et al. [1] demonstrate
that surface based brain mapping can offer advantages over volume based brain
mapping, especially when localizing cortical deficits and functional activations.
Thompson et al. [4,5] introduce a mathematical framework based on covariant
partial differential equations, and pull-backs of mappings under harmonic flows,
to help analyze signals localized on brain surfaces.

1.1   Previous Work

Conformal surface parameterizations have been studied intensively. Most works in conformal parameterizations deal with surface patches homeomorphic to topological disks. For surfaces with arbitrary topologies, Gu and Yau [6] introduce a general method for global conformal parameterizations based on the structure of the cohomology group of holomorphic one-forms. They generalize the method for surfaces with boundaries in [7].

For genus zero surfaces, there are five basic approaches to achieve conformal parameterizations.

1. *Harmonic energy minimization.* Eck et al. [8] introduce the discrete harmonic map, which approximates the continuous harmonic map [9] by minimizing a *metric dispersion* criterion. Desbrun et al. [10,11] compute the discrete Dirichlet energy and apply conformal parameterization to interactive geometry remeshing. Pinkall and Polthier compute the discrete harmonic map and Hodge star operator for the purpose of creating a minimal surface [12]. Kanai et al. use a harmonic map for geometric metamorphosis in [13]. Gu and Yau in [6] introduce a non-linear optimization method to compute global conformal parameterizations for genus zero surfaces. The optimization is carried out in the tangent spaces of the sphere.
2. *Cauchy-Riemann equation approximation.* Levy et al. [14] compute a quasi-conformal parameterization of topological disks by approximating the Cauchy-Riemann equation using the least squares method. They show rigorously that the quasi-conformal parameterization exists uniquely, and is invariant to similarity transformations, independent of resolution, and orientation preserving.
3. *Laplacian operator linearization.* Haker et al. [3] use a method to compute a global conformal mapping from a genus zero surface to a sphere by representing the Laplace-Beltrami operator as a linear system.
4. *Circle packing.* Circle packing is introduced in [2]. Classical analytic functions can be approximated using circle packing. But for general surfaces in $\mathbb{R}^3$, the circle packing method considers only the connectivity but not the geometry, so it is not suitable for our parameterization purpose.

Bakircioglu et al. use spherical harmonics to compute a flow on the sphere in [15] in order to match curves on the brain. Thompson and Toga use a similar approach in [16]. This flow field can be thought of as the variational minimizer of the integral over the sphere of Lu, with L some power of the Laplacian, and u the deformation. This is very similar to the spherical harmonic map used in this paper.

1.2   Basic Idea

It is well known that any genus zero surface can be mapped conformally onto the sphere and any local portion thereof onto a disk. This mapping, a conformal equivalence, is one-to-one, onto, and angle-preserving. Moreover, the elements

of the first fundamental form remain unchanged, except for a scaling factor (the so-called *Conformal Factor*). For this reason, conformal mappings are often described as being similarities in the small. Since the cortical surface of the brain is a genus zero surface, conformal mapping offers a convenient method to retain local geometric information, when mapping data between surfaces. Indeed, several groups have created flattened representations or visualizations of the cerebral cortex or cerebellum [2,3] using conformal mapping techniques. However, these approaches are either not strictly angle preserving [2], or there may be areas with large geometric distortions [3]. In this paper, we propose a new genus zero surface conformal mapping algorithm [6] and demonstrate its use in computing conformal mappings between brain surfaces. Our algorithm depends only on the surface geometry and is invariant to changes in image resolution and the specifics of data triangulation. Our experimental results show that our algorithm has advantageous properties for cortical surface matching.

Suppose K is a simplicial complex, and $f : |K| \to R^3$, which embeds $|K|$ in R^3; then (K, f) is called a mesh. Given two genus zero meshes M_1, M_2, there are many conformal mappings between them. Our algorithm for computing conformal mappings is based on the fact that for genus zero surfaces S_1, S_2, $f : S_1 \to S_2$ is conformal if and only if f is harmonic. All conformal mappings between S_1, S_2 form a group, the so-called Möbius group. Our method is as follows: we first find a homeomorphism h between M_1 and M_2, then deform h such that h minimizes the harmonic energy. To ensure the convergence of the algorithm, constraints are added; this also ensures that there is a unique conformal map.

This paper is organized as follows. In Section 2, we give the definitions of a piecewise linear function space, inner product and piecewise Laplacian. In Section 3, we describe the steepest descent algorithm which is used to minimize the string energy. In Section 4, we detail our conformal spherical mapping algorithms. Experimental results on conformal mapping for brain surfaces are reported in Section 6. In Section 7, we compare our algorithm with other conformal mapping approaches used in neuroimaging. We conclude the paper in Section 8.

2 Piecewise Linear Function Space, Inner Product, and Laplacian

For the diffeomorphisms between genus zero surfaces, if the map minimizes the harmonic energy, then it is conformal. Based on this fact, the algorithm is designed as a steepest descendent method.

Definition 1. *All piecewise linear functions defined on K form a linear space, denoted by $C^{PL}(K)$.*

Definition 2. *Suppose a set of string constants $k_{u,v}$ are assigned for each edge $\{u, v\}$, the inner product on C^{PL} is defined as the quadratic form*

$$< f, g > = \frac{1}{2} \sum_{\{u,v\} \in K} k_{u,v}(f(u) - f(v))(g(u) - g(v)) \tag{1}$$

The energy is defined as the norm on C^{PL}.

Definition 3. *Suppose $f \in C^{PL}$, the string energy is defined as:*

$$E(f) = <f, f> = \sum_{\{u,v\} \in K} k_{u,v} ||f(u) - f(v)||^2 \tag{2}$$

By changing the string constants $k_{u,v}$ in the energy formula, we can define different string energies.

Definition 4. *If string constants $k_{u,v} \equiv 1$, the string energy is known as the Tuette energy.*

Definition 5. *Suppose edge $\{u,v\}$ has two adjacent faces T_α, T_β, $T_\alpha = \{v_0, v_1, v_2\}$, define the parameters*

$$a_{v_1,v_2}^\alpha = \frac{1}{2} \frac{(v_1 - v_3) \cdot (v_2 - v_3)}{|(v_1 - v_3) \times (v_2 - v_3)|} \tag{3}$$

$$a_{v_2,v_3}^\alpha = \frac{1}{2} \frac{(v_2 - v_1) \cdot (v_3 - v_1)}{|(v_2 - v_1) \times (v_3 - v_1)|} \tag{4}$$

$$a_{v_3,v_1}^\alpha = \frac{1}{2} \frac{(v_3 - v_2) \cdot (v_1 - v_2)}{|(v_3 - v_2) \times (v_1 - v_2)|} \tag{5}$$

$$\tag{6}$$

T_β *is defined similarly. If $k_{u,v} = a_{u,v}^\alpha + a_{u,v}^\beta$, the string energy obtained is called the harmonic energy.*

The string energy is always a quadratic form. By carefully choosing the string coefficients, we make sure the quadratic form is positive definite. This will guarantee the convergence of the steepest descent method.

Definition 6. *The piecewise Laplacian is the linear operator $\Delta_{PL} : C^{PL} \to C^{PL}$ on the space of piecewise linear functions on K, defined by the formula*

$$\Delta_{PL}(f) = \sum_{\{u,v\} \in K} k_{u,v}(f(v) - f(u)) \tag{7}$$

If f minimizes the string energy, then f satisfies the condition $\Delta_{PL}(f) = 0$. Suppose M_1, M_2 are two meshes and the map $\boldsymbol{f} : M_1 \to M_2$ is a map between them, $\boldsymbol{f}$ can be treated as a map from M_1 to R^3 also.

Definition 7. *For a map $\boldsymbol{f} : M_1 \to R^3$, $\boldsymbol{f} = (f_0, f_1, f_2)$, $f_i \in C^{PL}, i = 0, 1, 2$, we define the energy as the norm of $\boldsymbol{f}$:*

$$E(\boldsymbol{f}) = \sum_{i=0}^{2} E(f_i) \tag{8}$$

The Laplacian is defined in a similar way,

Definition 8. *For a map $\boldsymbol{f} : M_1 \to R^3$, the piecewise Laplacian of $\boldsymbol{f}$ is*

$$\Delta_{PL}\boldsymbol{f} = (\Delta_{PL}f_0, \Delta_{PL}f_1, \Delta_{PL}f_2) \tag{9}$$

A map $\boldsymbol{f} : M_1 \to M_2$ is harmonic, if and only if $\Delta_{PL}\boldsymbol{f}$ only has a normal component, and its tangential component is zero.

$$\Delta_{PL}(\boldsymbol{f}) = (\Delta_{PL}\boldsymbol{f})^{\perp} \tag{10}$$

3   Steepest Descent Algorithm

Suppose we would like to compute a mapping $\boldsymbol{f} : M_1 \to M_2$ such that $\boldsymbol{f}$ minimizes a string energy $E(\boldsymbol{f})$. This can be solved easily by the steepest descent algorithm:

$$\frac{d\boldsymbol{f}(t)}{dt} = -\Delta\boldsymbol{f}(t) \tag{11}$$

$\boldsymbol{f}(M_1)$ is constrained to be on M_2, so $-\Delta\boldsymbol{f}$ is a section of M_2's tangent bundle.

Specifically, suppose $\boldsymbol{f} : M_1 \to M_2$, and denote the image of each vertex $v \in K_1$ as $\boldsymbol{f}(v)$. The normal on M_2 at $\boldsymbol{f}(v)$ is $\boldsymbol{n}(\boldsymbol{f}(v))$. Define the normal component as

Definition 9. *The normal component*

$$(\Delta\boldsymbol{f}(v))^{\perp} = <\Delta\boldsymbol{f}(v), \boldsymbol{n}(\boldsymbol{f}(v)) > \boldsymbol{n}(\boldsymbol{f}(v)), \tag{12}$$

where $<,>$ is the inner product in R^3.

Definition 10. *The absolute derivative is defined as*

$$D\boldsymbol{f}(v) = \Delta\boldsymbol{f}(v) - (\Delta\boldsymbol{f}(v))^{\perp} \tag{13}$$

Then equation (14) is $\delta\boldsymbol{f} = -D\boldsymbol{f} \times \delta t$.

4   Conformal Spherical Mapping

Suppose M_2 is S^2, then a conformal mapping $\boldsymbol{f} : M_1 \to S^2$ can be constructed by using the steepest descent method. The major difficulty is that the solution is not unique but forms a Möbius group.

Definition 11. *Mapping $f : C \to C$ is a Möbius transformation if and only if*

$$f(z) = \frac{az + b}{cz + d}, \ \ a, b, c, d \in C, ad - bc \neq 0 \tag{14}$$

All Möbius transformations form the Möbius transformation group. In order to determine a unique solution we can add different constraints. In practice we use the following two constraints: the zero mass-center constraint and a landmark constraint.

Definition 12. *Mapping $\boldsymbol{f} : M_1 \to M_2$ satisfies the zero mass-center condition if and only if*

$$\int_{M_2} \boldsymbol{f} d\sigma_{M_1} = 0, \tag{15}$$

where σ_{M_1} is the area element on M_1.

All conformal maps from M_1 to S^2 satisfying the zero mass-center constraint are unique up to a Euclidean rotation group (which is 3 dimensional). We use the Gauss map as the initial condition.

Definition 13. *A Gauss map $N : M_1 \to S^2$ is defined as*

$$N(v) = \boldsymbol{n}(v), v \in M_1, \tag{16}$$

$\boldsymbol{n}(v)$ *is the normal at v.*

Algorithm 1 *Spherical Tuette Mapping*

Input (mesh M, step length δt, energy difference threshold δE), output($\boldsymbol{t}$: $M \to S^2$) where $\boldsymbol{t}$ minimizes the Tuette energy.

1. *Compute Gauss map $N : M \to S^2$. Let $\boldsymbol{t} = N$, compute Tuette energy E_0.*
2. *For each vertex $v \in M$, compute Absolute derivative $D\boldsymbol{t}$.*
3. *Update $\boldsymbol{t}(v)$ by $\delta\boldsymbol{t}(v) = -D\boldsymbol{t}(v)\delta t$.*
4. *Compute Tuette energy E.*
5. *If $E - E_0 < \delta E$, return $\boldsymbol{t}$. Otherwise, assign E to E_0 and repeat steps 2 through to 5.*

Because the Tuette energy has a unique minimum, the algorithm converges rapidly and is stable. We use it as the initial condition for the conformal mapping.

Algorithm 2 *Spherical Conformal Mapping*

Input (mesh M, step length δt, energy difference threshold δE), output($\boldsymbol{h}$: $M \to S^2$). Here $\boldsymbol{h}$ minimizes the harmonic energy and satisfies the zero mass-center constraint.

1. *Compute Tuette embedding $\boldsymbol{t}$. Let $\boldsymbol{h} = \boldsymbol{t}$, compute Tuette energy E_0.*
2. *For each vertex $v \in M$, compute the absolute derivative $D\boldsymbol{h}$.*
3. *Update $\boldsymbol{h}(v)$ by $\delta\boldsymbol{h}(v) = -D\boldsymbol{h}(v)\delta t$.*
4. *Compute Möbius transformation $\boldsymbol{\varphi}_0 : S^2 \to S^2$, such that*

$$\Gamma(\boldsymbol{\varphi}) = \int_{S^2} \boldsymbol{\varphi} \circ \boldsymbol{h} d\sigma_{M_1}, \boldsymbol{\varphi} \in Mobius(CP^1) \tag{17}$$

$$\boldsymbol{\varphi}_0 = \min_{\boldsymbol{\varphi}} ||\Gamma(\boldsymbol{\varphi})||^2 \tag{18}$$

where σ_{M_1} is the area element on M_1. $\Gamma(\boldsymbol{\varphi})$ is the mass center, $\boldsymbol{\varphi}$ minimizes the norm of mass center.

5. *compute the harmonic energy E.*
6. *If $E - E_0 < \delta E$, return $\boldsymbol{t}$. Otherwise, assign E to E_0 and repeat step 2 through to step 6.*

Step 4 is non-linear and expensive to compute. In practice we use the following procedure to replace it:

1. Compute the mass center $\boldsymbol{c} = \int_{S^2} \boldsymbol{h} d\sigma_{M_1}$;
2. For all $v \in M$, $\boldsymbol{h}(v) = \boldsymbol{h}(v) - \boldsymbol{c}$;
3. For all $v \in M$, $\boldsymbol{h}(v) = \frac{\boldsymbol{h}(v)}{||\boldsymbol{h}(v)||}$.

This approximation method is good enough for our purpose. By choosing the step length carefully, the energy can be decreased monotonically at each iteration.

5   Optimize the Conformal Parameterization by Landmarks

In order to compare two brain surfaces, it is desirable to adjust the conformal parameterization and match the geometric features on the brains as well as possible. We define an energy to measure the quality of the parameterization. Suppose two brain surfaces S_1, S_2 are given, conformal parameterizations are denoted as $f_1 : S^2 \to S_1$ and $f_2 : S^2 \to S_2$, the *matching energy* is defined as

$$E(f_1, f_2) = \int_{S^2} ||f_1(u, v) - f_2(u, v)||^2 dudv \qquad (19)$$

We can composite a Möbius transformation τ with f_2, such that

$$E(f_1, f_2 \circ \tau) = \min_{\zeta \in \Omega} E(f_1, f_2 \circ \zeta), \qquad (20)$$

where Ω is the group of Möbius transformations. We use landmarks to obtain the optimal Möbius transformation. Landmarks are commonly used in brain mapping. We manually label the landmarks on the brain as a set of sulcal curves [4], as shown in Figure 5. First we conformally map two brains to the sphere, then we pursue a best Möbius transformation to minimize the Euclidean distance between the corresponding landmarks on the spheres. Suppose the landmarks are represented as discrete point sets, and denoted as $\{p_i \in S_1\}$ and $\{q_i \in S_2\}$, p_i matches q_i, $i = 1, 2, \ldots, n$. The landmark mismatch functional for $u \in \Omega$ is defined as

$$E(u) = \sum_{i=1}^{n} ||p_i - u(q_i)||^2, u \in \Omega, p_i, q_i \in S^2 \qquad (21)$$

In general, the above variational problem is a nonlinear one. In order to simplify it, we convert it to a least squares problem. First we project the sphere to the complex plane, then the Möbius transformation is represented as a complex linear rational formula, Equation 14. We add another constraint for u, so that u maps infinity to infinity. That means the north poles of the spheres are mapped

to each other. Then u can be represented as a linear form $az + b$. Then the functional of u can be simplified as

$$E(u) = \sum_{i=1}^{n} g(z_i)|az_i + b - \tau_i|^2 \tag{22}$$

where z_i is the stereo-projection of p_i, τ_i is the projection of q_i, g is the conformal factor from the plane to the sphere, it can be simplified as

$$g(z) = \frac{4}{1 + z\bar{z}}. \tag{23}$$

So the problem is a least squares problem.

6   Experimental Results

The 3D brain meshes are reconstructed from 3D 256x256x124 T1 weighted SPGR (spoiled gradient) MRI images, by using an active surface algorithm that deforms a triangulated mesh onto the brain surface [5]. Figure 1(a) and (c) show the same brain scanned at different times [4]. Because of the inaccuracy introduced by scanner noise in the input data, as well as slight biological changes over time, the geometric information is not exactly the same. Figure 1(a) and (c) reveal minor differences.
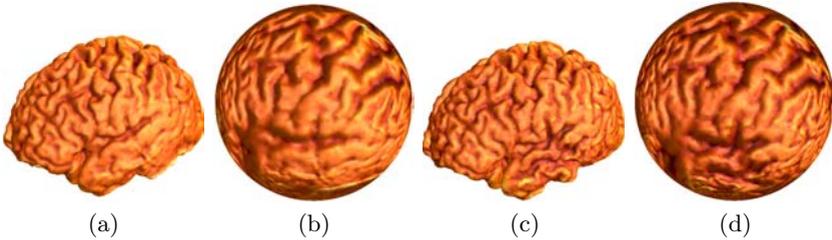

(a)   (b)   (c)   (d)

Fig. 1. Reconstructed brain meshes and their spherical harmonic mappings. (a) and (c) are the reconstructed surfaces for the same brain scanned at different times. Due to scanner noise and inaccuracy in the reconstruction algorithm, there are visible geometric differences. (b) and (d) are the spherical conformal mappings of (a) and (c) respectively; the normal information is preserved. By the shading information, the correspondence is illustrated.

The conformal mapping results are shown in Figure 1(b) and (d). From this example, we can see that although the brain meshes are slightly different, the mapping results look quite similar. The major features are mapped to the same position on the sphere. This suggests that the computed conformal mappings continuously depend on the geometry, and can match the major features consistently and reproducibly. In other words, conformal mapping may be a good candidate for a canonical parameterization in brain mapping.
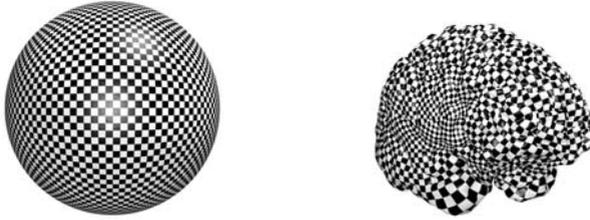
(a) Texture mapping of the sphere (b) Texture mapping of the brain

Fig. 2. Conformal texture mapping. The conformality is visualized by texture mapping of a checkerboard image. The sphere is mapped to the plane by stereographic projection, then the planar coordinates are used as the texture coordinates. This texture parameter is assigned to the brain surface through the conformal mapping between the sphere and the brain surface. All the right angles on the texture are preserved on the brain surface.
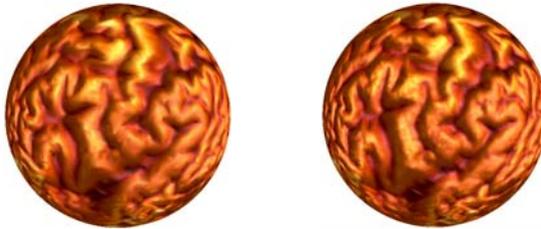
(a) Surface with 20,000 faces (b) Surface with 50,000 faces

Fig. 3. Conformal mappings of surfaces with different resolutions. The original brain surface has 50,000 faces, and is conformally mapped to a sphere, as shown in (a). Then the brain surface is simplified to 20,000 faces, and its spherical conformal mapping is shown in (b).
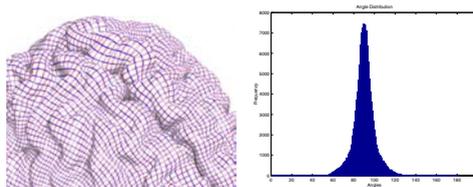
(a) Intersection angles (b) Angle distribution

Fig. 4. Conformality measurement. The curves of iso-polar angle and iso-azimuthal angle are mapped to the brain, and the intersection angles are measured on the brain. The histogram is illustrated.
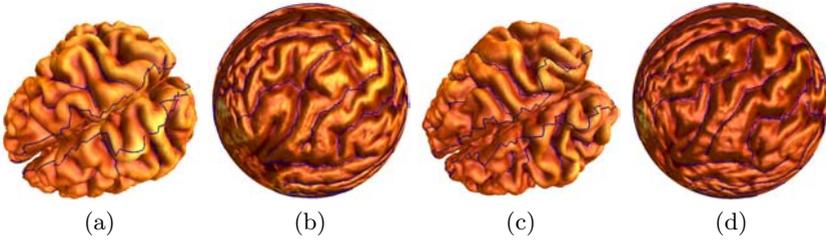
(a)   (b)   (c)   (d)

Fig. 5. Möbius transformation to minimize the deviations between landmarks. The blue curves are the landmarks. The correspondence between curves has been preassigned. The desired Möbius transformation is obtained to minimize the matching error on the sphere.
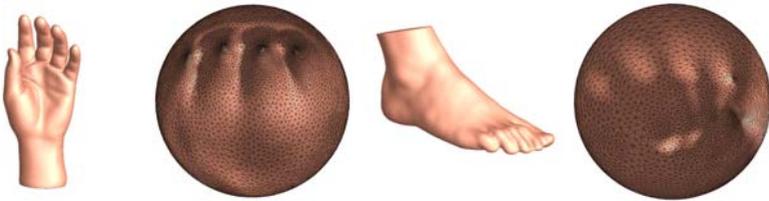

Fig. 6. Spherical conformal mapping of genus zero surfaces. Extruding parts (such as fingers and toes) are mapped to denser regions on the sphere.

Figure 2 shows the mapping is conformal by texture mapping a checker board to both the brain surface mesh and a spherical mesh. Each black or white square in the texture is mapped to sphere by stereographic projection, and pulled back to the brain. Note that the right angles are preserved both on the sphere and the brain.

Conformal mappings are stable and depend continuously on the input geometry but not on the triangulations, and are insensitive to the resolutions. Figure 3 shows the same surface with different resolutions, and their conformal mappings. The mesh simplification is performed using a standard method. The refined model has 50k faces, coarse one has 20k faces. The conformal mappings map the major features to the same positions on the spheres.

In order to measure the conformality, we map the iso-polar angle curves and iso-azimuthal angle curves from the sphere to the brain by the inverse conformal mapping, and measure the intersection angles on the brain. The distribution of the angles of a subject(A) are illustrated in Figure 4. The angles are concentrated about the right angle.

Figure 5 shows the landmarks, and the result of the optimization by a Möbius transformation. We also computed the matching energy, following Equation 19. We did our testing among three subjects. Their information is shown in Table 1. We took subject A as the target brain. For each new subject model, we found a Möbius transformation that minimized the landmark mismatch energy on the

maximum intersection subsets of it and A. As shown in Table 1, the matching energies were reduced after the Möbius transformation.

The method described in this work is very general. We tested the algorithm on other genus zero surfaces, including the hand and foot surface. The results are illustrated in Figure 6.

7   Comparison with Other Work

Several other studies of conformal mappings between brain surfaces are reported in [2,3]. In [2], Hurdal et al. used the circle packing theorem and the ring lemma to establish a theorem: there is a unique circle packing in the plane (up to certain transformations) which is quasi-conformal (i.e. angular distortion is bounded) for a simply-connected triangulated surface. They demonstrated their experimental results for the surface of the cerebellum. This method only considers the topology without considering the brain's geometric structure. Given two different mesh structures of the same brain, one can predict that their methods may generate two different mapping results. Compared with their work, our method really preserves angles and establishes a good mapping between brains and a canonical space.

Haker et al. [3] built a finite element approximation of the conformal mapping method for brain surface parameterization. They selected a point as the north pole and conformally mapped the cortical surface to the complex plane. In the resulting mapping, the local shape is preserved and distances and areas are only changed by a scaling factor. Since stereo projection is involved, there is significant distortion around the north pole areas, which brings instability to this approach. Compared with their work, our method is more accurate, with no regions of large area distortion. It is also more stable and can be readily extended to compute maps between two general manifolds.

Finally, we note that Memoli et al. [17] mentioned they were developing implicit methods to compute harmonic maps between general source and target manifolds. They used level sets to represent the brain surfaces. Due to the extensive folding of the human brain surface, these mappings have to be designed very carefully.

Table 1. Matching energy for three subjects. Subject A was used as the target brain. For subjects B and C, we found Möbius transformations that minimized the landmark mismatch functions, respectively.

Subject	Vertex #	Face #	Before	After
A	65,538	131,072	-	-
B	65,538	131,072	604.134	506.665
C	65,538	131,072	414.803	365.325

8   Conclusion and Future Work

In this paper, we propose a general method which finds a unique conformal mapping between genus zero manifolds. Specifically, we demonstrate its feasibility for brain surface conformal mapping research. Our method only depends on the surface geometry and not on the mesh structure (i.e. gridding) and resolution. Our algorithm is very fast and stable in reaching a solution. There are numerous applications of these mapping algorithms, such as providing a canonical space for automated feature identification, brain to brain registration, brain structure segmentation, brain surface denoising, and convenient surface visualization, among others. We are trying to generalize this approach to compute conformal mappings between nonzero genus surfaces.

References

1. B. Fischl, M.I. Sereno, R.B.H. Tootell, and A.M. Dale. High-resolution inter-subject averaging and a coordinate system for the cortical surface. In *Human Brain Mapping*, volume 8, pages 272–284, 1999.
2. M.K. Hurdal, K. Stephenson, P.L. Bowers, D.W.L. Sumners, and D.A. Rottenberg. Coordinate systems for conformal cerebellar flat maps. In *NeuroImage*, volume 11, page S467, 2000.
3. S. Haker, S. Angenent, A. Tannenbaum, R. Kikinis, G. Sapiro, and M. Halle. Conformal surface parameterization for texture mapping. *IEEE Transactions on Visualization and Computer Graphics*, 6(2):181–189, April-June 2000.
4. P.M. Thompson, M.S. Mega, C. Vidal, J.L. Rapoport, and A.W. Toga. Detecting disease-specific patterns of brain structure using cortical pattern matching and a population-based probabilistic brain atlas. In *Proc. 17th International Conference on Information Processing in Medical Imaging (IPMI2001)*, pages 488–501, Davis, CA, USA, June 18–22 2001.
5. P.M. Thompson and A.W. Toga. A framework for computational anatomy. In *Computing and Visualization in Science*, volume 5, pages 1–12, 2002.
6. X. Gu and S. Yau. Computing conformal structures of surfaces. *Communications in Information and Systems*, 2(2):121–146, December 2002.
7. X. Gu and S. Yau. Global conformal surface parameterization. *preprint*, December 2002.
8. M. Eck, T. DeRose, T. Duchamp, H. Hoppe, M. Lounsbery, and W. Stuetzle. Multiresolution analysis of arbitrary meshes. In *Computer Graphics (Proceedings of SIGGRAPH 95)*, August 1995.
9. R. Schoen and S.T. Yau. *Lectures on Harmonic Maps.* International Press, Harvard University, Cambridge MA, 1997.
10. P. Alliez, M. Meyer, and M. Desbrun. Interactive geometry remeshing. In *Computer Graphics (Proceedings of SIGGRAPH 02)*, pages 347–354, 2002.
11. M. Desbrun, M. Meyer, and P. Alliez. Intrinsic parametrizations of surface meshes. In *Proceedings of Eurographics*, 2002.
12. U. Pinkall and K. Polthier. Computing discrete minimal surfaces and their conjugates. In *Experim. Math.*, volume 2(1), pages 15–36, 1993.
13. T. Kanai, H. Suzuki, and F. Kimura. Three-dimensional geometric metamorphosis based on harmonic maps. *The Visual Computer*, 14(4):166–176, 1998.

14. B. Levy, S. Petitjean, N. Ray, and J. Maillot. Least squares conformal maps for automatic texture atlas generation. In *Computer Graphics (Proceedings of SIGGRAPH 02)*. Addison Wesley, 2002.
15. M. Bakircioglu, U. Grenander, N. Khaneja, and M.I. Miller. Curve matching on brain surfaces using frenet distances. *Human Brain Mapping*, 6:329–333, 1998.
16. P. Thompson and A. Toga. A surface-based technique for warping 3-dimensional images of the brain. *IEEE Transactions on Medical Imaging*, 15(4):1–16, 1996.
17. F. Memoli, G. Sapiro, and S. Osher. Solving variational problems and partial equations mapping into general target manifolds. Technical Report 02–04, CAM Report, January 2002.